Nanoscale Res Lett (2010) 5:686–691
DOI 10.1007/s11671-010-9532-2

NANO EXPRESS

Oxygen Absorption in Free-Standing Porous Silicon: A Structural, Optical and Kinetic Analysis

Rodolfo Cisneros · Heriberto Pfeiffer · Chumin Wang

Received: 27 November 2009 / Accepted: 5 January 2010 / Published online: 16 January 2010

Abstract Porous silicon (PSi) is a nanostructured material possessing a huge surface area per unit volume. In consequence, the adsorption and diffusion of oxygen in PSi are particularly important phenomena and frequently cause significant changes in its properties. In this paper, we study the thermal oxidation of p^+-type free-standing PSi fabricated by anodic electrochemical etching. These free-standing samples were characterized by nitrogen adsorption, thermogravimetry, atomic force microscopy and powder X-ray diffraction. The results show a structural phase transition from crystalline silicon to a combination of cristobalite and quartz, passing through amorphous silicon and amorphous silicon-oxide structures, when the thermal oxidation temperature increases from 400 to 900 °C. Moreover, we observe some evidence of a sinterization at 400 °C and an optimal oxygen-absorption temperature about 700 °C. Finally, the UV/Visible spectrophotometry reveals a red and a blue shift of the optical transmittance spectra for samples with oxidation temperatures lower and higher than 700 °C, respectively.

Keywords Porous silicon · Thermal oxidation · Kinetic analysis · Structural transition · Optical properties

R. Cisneros · H. Pfeiffer · C. Wang (✉)
Instituto de Investigaciones en Materiales, Universidad Nacional Autónoma de México, Circuito Exterior s/n, Ciudad Universitaria, Del. Coyoacán, Apartado Postal 70-360, 04510 Mexico D.F., Mexico
e-mail: chumin@servidor.unam.mx

Introduction

Silicon, being the second most abundant element in the Earth's crust after oxygen, is the base of nowadays microelectronics. However, all-silicon optoelectronic devices are still a challenger, since the bulk crystalline silicon (*c*-Si) has an indirect band gap of 1.1 eV, which inhibits efficient optical interband transitions. In 1990, L.T. Canham reported the first observation of a surprising visible photoluminescence at room temperature in porous silicon (PSi) [1], originated from its nanostructured *c*-Si skeleton. In consequence, as many other porous nanomaterials [2–4], PSi is expected to have a wide range of photonic and biologic applications, mainly arising from its tunable refractive index [5], biocompatibility [6] and large surface/volume ratio [7]. Nevertheless, this large surface area makes PSi chemically unstable, and its oxidation is a common natural process. In fact, the storage of PSi samples in ambient air makes important changes in its electrical and optical properties [8, 9]. Porous materials can be thermally oxidized through different methods [10]. Specifically, the thermal oxidation of PSi under controlled temperature and oxygen atmosphere shows an increase in the surface roughness at 200–400 °C and a decrease at 600–800 °C [11]. Furthermore, the *ac* electrical conductivity of oxidized PSi reveals two power-law behaviors at mid and high temperatures, suggesting a two-stage oxidation picture [12]. Also, PSi structural modifications during its formation have been investigated in situ by X-ray diffractions (XRD) revealing a lattice expansion [13], which is consistent with quantum mechanical calculations [14]. In general, the PSi samples present narrow diffraction peaks and constitute a rare example of a porous structure inside a nearly perfect single crystal. In this paper, we report a multi-approach study of the thermal oxidation in PSi by correlating the

oxygen-absorption process with their structural and optical properties. The results suggest the existence of an unusual temperature about 700 °C, where both an optimal oxygen absorption and a structural phase transition occur. In fact, the measured optical transmittance spectra obtained from thermally oxidized free-standing PSi samples seem to confirm this structural phase transition.

Experimental Setup

The PSi samples used in this study were fabricated by means of an anodic electrochemical dissolution of boron-doped p^+-type (100)-oriented *c*-Si wafers with an electrical resistivity of 0.01–0.03 Ω cm in an electrolyte consisting of a mixture of HF (49%) and ethanol (99.9%) with a volume ratio of 1:2 [15]. A gold film of 30 nm was deposited on the backside of *c*-Si wafers to ensure electrical conduction during the anodization. In the course of etching process, a *dc* electrical current of 25 mA/cm^2 for 200 s was applied between the platinum electrode and the wafer backside contact. To remove the PSi layer from the wafer, an additional *dc* current of 376 mA/cm^2 for 10 s was following applied, producing a free-standing PSi film with a thickness of 7.5–8.5 μm measured by optical and scanning electron microscopies. The electrolyte was recycled by a mechanical pump to remove air bubbles generated by the electrochemical reaction and to improve the homogeneity of PSi thin films, where the etched area was approximately 2.9 cm^2. After etching, the samples were rinsed with ethanol, and those samples for optical measurements were put on slides of quartz.

The surface area of the samples was determined by the nitrogen-adsorption technique [16]. These samples were fragmented into grains with an average diameter of 3 mm. The N_2 adsorption–desorption isotherms were measured at 77 K using a Belsorp-Mini II gas adsorption analyzer from BEL Japan. Before the N_2 adsorption process, samples were outgassed with a vacuum of 0.1 mbar at room temperature for 12 h. The specific surface area was calculated by means of the Langmuir and BET equations [17], while the pore diameters were estimated through the BJH model [18].

Later, these fragmented PSi samples were characterized by the thermogravimetric analysis (TGA) by means of a Q500HR thermobalance from TA Instruments. In particular, one of the samples was dynamically analyzed from the room temperature to 900 °C at a speed of 3 °C/min, within an O_2 flux of 60 ml/min. Other 10 samples were isothermically studied at different temperatures with the same O_2 flux. These samples were subsequently analyzed by the powder XRD, whose patterns were obtained from a Bruker AXS D8 Advance X-ray diffractometer using a $K_{\alpha 1}$ wavelength of 1.5406 Å. The microstructures were identified using the Joint Compounds Powder Diffraction Standards (JCPDS) database. In addition, the surface nanoscale morphology of the samples was examined by the Atomic Force Microscopy (AFM) using a scanning probe microscope (JEOL JSPM-4210) with a NSC12/50 silicon tip in the tapping mode.

On the other hand, the quartz-slide-mounted free-standing PSi samples were thermally oxidized at temperatures of 100, 300, 500, 700, 800 and 900 °C in an ultra-dry oxygen atmosphere for 30 min using a Carbolite horizontal electric tube furnace. The optical transmission spectra of these samples were recorded with a Varian Cary 100 UV–Vis double-beam spectrophotometer at room temperature and atmospheric pressure.

Results and Discussion

The surface area and pore diameter of the samples were determined by nitrogen adsorption. Figure 1 shows the N_2 adsorption–desorption isotherm by plotting the adsorbed volume as a function of the gas pressure (P) normalized by the adsorptive saturation pressure at 77 K (P_0). The results reveal an isotherm of type IV accompanied by a type-H1 hysteresis loop according to the International Union of Pure and Applied Chemistry (IUPAC) [16]. This type of isotherms is distinctive of mesoporous materials with a pore diameter of 2–50 nm and a high energy of adsorption, while the H1-type hysteresis is generally associated to regular pores with almost non-interconnecting channels [16]. Furthermore, the experimental data were fitted using the BJH model [18], and the pore size distribution is presented in the inset of Fig. 1, which indicates an average

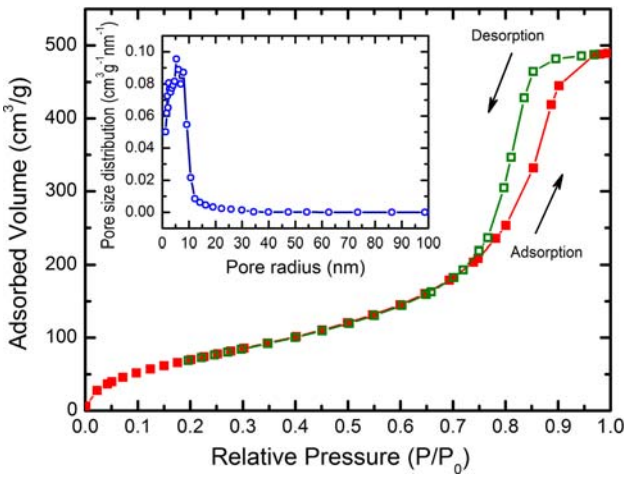

Fig. 1 N_2 adsorption (*solid squares*) and desorption (*open squares*) isotherms at 77 K plotted as a function of the gas pressure (*P*) normalized by the adsorptive saturation pressure (P_0). *Inset* BJH pore size distribution derived from the N_2 sorption isotherms

pore radius about 5.3 nm. Likewise, the analysis of surface area through Langmuir and BET methods [17], respectively, leads to 285.7 and 283.8 m^2/g. These observations of porous morphology are in good agreement with previous reports [19, 20].

Once the structural characteristics of the samples were determined, a thermogravimetric analysis (TGA) was performed at different temperatures in order to elucidate the kinetics of oxygen absorption in free-standing PSi (Fig. 2). Firstly, a sample was dynamically analyzed using the thermobalance described in the previous section, and its thermogram is presented in Fig. 2a, in which the sample began to increase its weight over 180 °C, since under that temperature a humidity evaporation seems to occur. Note that this increment of weight did not stop in the whole analyzed temperature range with a maximum weight-increase rate around 750 °C and achieves a total weight increase of 58 wt%. All this increment of weight can be attributed to two different processes; adsorption and/or absorption. In particular, the effects of absorption can be determined by XRD, as shown below, revealing the formation of different SiO_2 phases of following reaction.

$$Si + O_2 \rightarrow SiO_2. \quad (1)$$

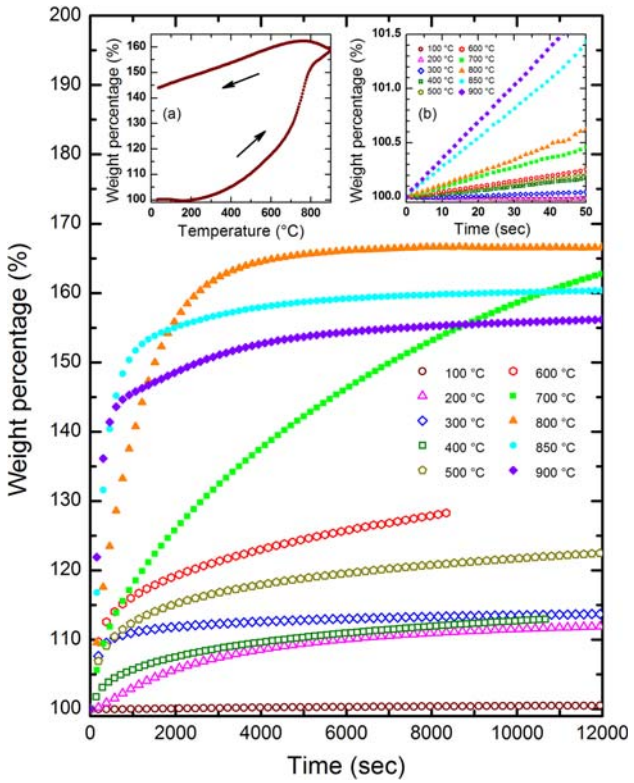

Fig. 2 Thermogravimetric analysis (*TGA*) isotherms of oxygen absorption at different temperatures indicated in the figure. *Insets a* dynamic oxygen-absorption TGA curve and *b* magnification of TGA isotherms for the first 50 s

Conversely, the adsorption process would be understood from the same dynamic TGA, specifically, from the cooling process. In this part of the thermogram, the sample loosed around of 10 wt% between 800 and 30 °C, which may be associated with some kind of oxygen adsorption. Hence, the final weight increment was 44 wt%. However, considering that the PSi surface area was 285.7 m^2/g and O_2 ionic diameter was 2.8 Å, the final weight increase must be equal to 24.6 wt% if single monolayer absorption of O_2 molecules was produced. Therefore, it should be assumed that oxygen is not only absorbed over the PSi surface, but also in its bulk as well. This result implies the existence of a diffusion process.

In order to further understand the oxygen absorption in PSi, different isotherms were measured as shown in Fig. 2, where the curve at 600 °C was truncated by a loss of mass during the measurement due to volume expansion of an excessive probing mass. From reaction 1, it can be deduced that a total conversion reaction in bulk implies an increment of weight of 214.3 wt%. None of the isotherms reached this value; the highest increased weight was 166 wt% for the isotherm performed at 800 °C. Moreover, from Fig. 2b, it can be seen that, at short times, all the isotherms follow a uniform absorption trend, i.e., a larger absorption corresponds to a higher temperature isotherm. However, at long time, isotherms presented two important variations: (1) Sample treated at 400 °C absorbed less O_2 than that at 300 °C for long time scale and (2) Samples treated at 700 and 800 °C seem to absorb more O_2 than those at 850 °C or higher temperatures. From previous works of gas absorption at different temperatures, it has been found that the sinterization could significantly modify the isotherm results [21]. Therefore, in order to elucidate whether a similar process is taking place in PSi samples, an AFM study was performed. An as-etched sample was heated at 500 °C during 4 h under an atmosphere of Ar, and its AFM image is presented in Fig. 3b, in comparison with Fig. 3a obtained from a sample without such heating treatment, where the color tones indicate the vertical scale of roughness. Notice that there is a clear difference between these two structures, i.e., the average diameters of both clusters of atoms and pores in Fig. 3b are significantly larger than those of Fig. 3a, which suggest a possible sintering process occurred around 400–500 °C. In fact, sintering of PSi seems to be unavoidable if it is processed at temperatures above 350 °C [22, 23]. It would be worth mentioning that the pore diameter of 10 nm observed in Fig. 3a is very close to the average pore radius of 5.3 nm revealed by the N_2 adsorption experiment.

Coming back to the isothermal analysis, the different variations observed in the isotherms can be explained as follows. First, at short times, the oxidation process occurs over the PSi surface, and the sintering effect and the

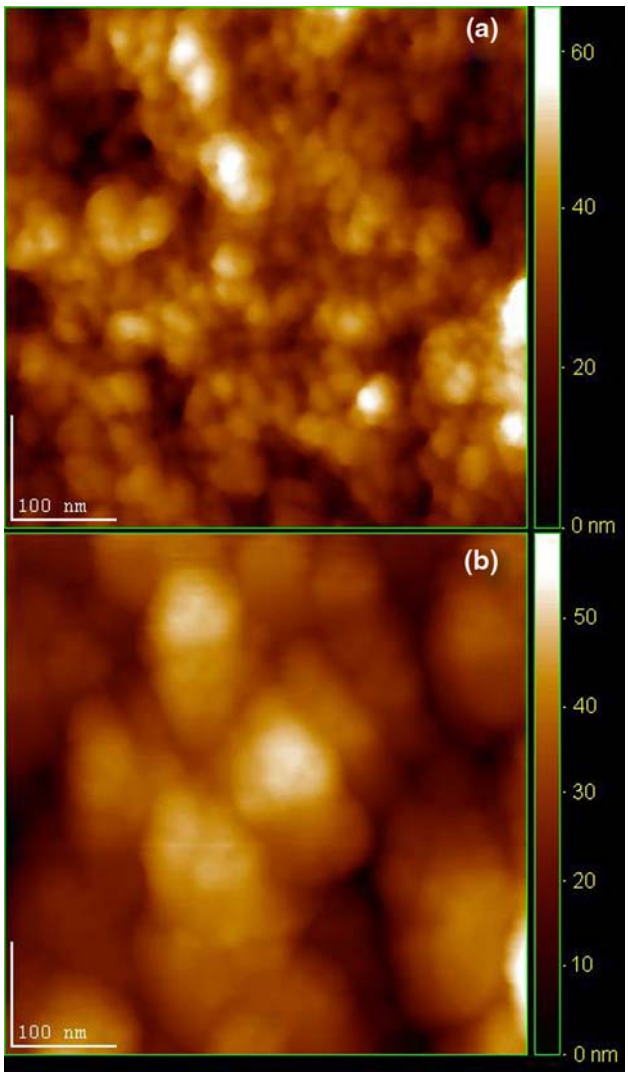

Fig. 3 Atomic force micrographs of the samples **a** without any heat treatment and **b** with a heat treatment at 500 °C under Ar flux for 4 h. The *color tones* indicate the vertical scale of roughness

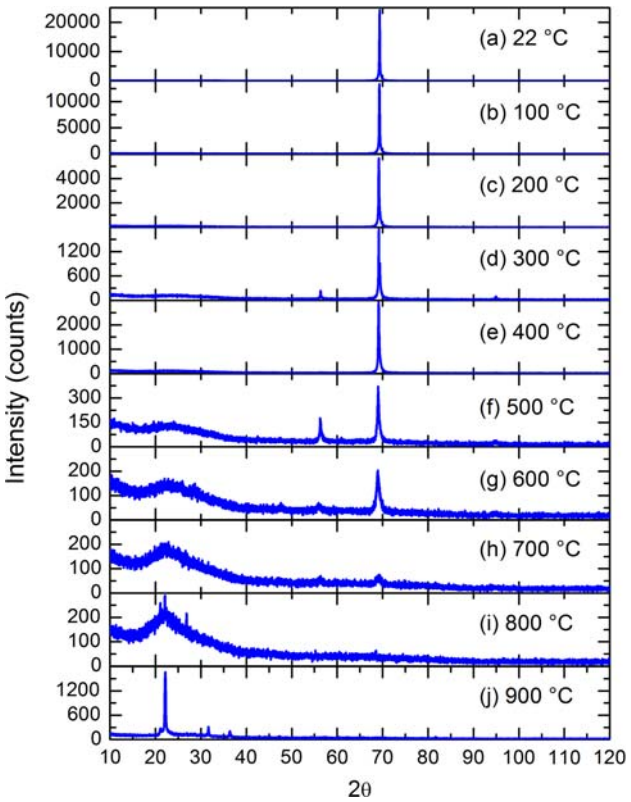

Fig. 4 **b–j** X-ray diffraction patterns corresponding to samples of Fig. 2 in comparison with **a** that pattern obtained from a sample without any heat treatment

diffusion process do not interfere. It explains why at short times the isotherms present a uniform trend. However, the sample treated at 400 °C presented an atypical behavior at long times due to the sintering process. Around that temperature, the surface has reacted but the diffusion of oxygen is still a less important process. In other words, the sample treated at 400 °C has a smaller amount of surface area than that at 300 °C, decreasing the O_2 absorbed. For higher temperatures, sintering must be enhanced. However, in these cases, sintering does not affect so importantly, since the diffusion process is becoming dominant. In the region of very high temperatures around 850–900 °C, a new equilibrium between surface absorption and desorption should be considered, since the oxygen desorption process is exponentially enhanced with the temperature, as stated in the Langmuir equation [17]. Therefore, an optimal oxygen-absorption temperature at 700 °C is found in Fig. 2.

After the TGA analysis, the same samples were characterized by XRD, including one without any thermal treatments. The diffraction pattern of this sample is shown in Fig. 4a, which could be fitted to the JCPDS file 27-1402. This file corresponds to a crystalline face-centered cubic Si structure. It should be pointed out that only the (004) diffraction peak ($2\theta = 69.1°$) was observed, which indicates that this material is totally oriented over the (001) family planes. Samples thermally treated at 100 and 200 °C did not seem to present any significant structural change, in comparison to the untreated sample. Nevertheless, the XRD pattern intensities of these samples decreased, which would be assumed as certain loss of crystallinity, except the pattern (e) at 400 °C. This exception could be related to the sintering process, since it may produce larger clusters of Si atoms and then more coherent (001) diffraction planes in the bulk. The XRD pattern of the sample heat treated at 300 °C presented two new diffraction peaks located at $2\theta = 56.2°$ and 94.9°, which could be fitted as well to the JCPDS-27-1402 file and correspond to (311) and (511) planes, respectively. This result indicates that PSi sample has started a policrytalization process at 300 °C or in other words, the preferential orientation is not totally preserved

under these thermal conditions. Furthermore, at low 2θ values (between 6° and 35°), this sample begins to depict some kind of amorphization. All these results and tendencies are dramatically increased as a function of the temperature, from 300 to 700 °C, where mixtures of crystalline and amorphous structures are observed. While the initially preferential oriented *c*-Si tends to disappear and to become polycrystalline, two different amorphous structures come into sight. These amorphous structures can be associated with the Si amorphization, signals observed between 6° and 15°, and amorphous SiO_2 formation (15°–35°), through an oxidation reaction. Although it was not quantitatively determined, the relationship between different phases seems to indicate that amorphous SiO_2 growths while amorphous Si (*a*-Si) and *c*-Si phases disappear. All these results and observations are corroborated on the samples heat treated at 800 and 900 °C, where *c*-Si has completely disappeared and new crystalline phases were detected. These crystalline phases correspond to quartz (JCPDS 070-3755) and cristobalite (JCPDS 39-1425), both belong crystalline structures of SiO_2. It would be pointed out that *a*-Si practically disappears at 900 °C.

Finally, the optical properties of free-standing PSi samples were characterized as well. In an ultra-dry oxygen atmosphere, these quartz-slide-mounted samples were thermally oxidized for 30 min at temperatures of 100, 300, 500, 700, 800 and 900 °C, and their optical transmission spectra are respectively shown in Fig. 5a–f. Observe that there is a critical wavelength (λ_c) in each figure and for $\lambda < \lambda_c$, the optical transmittance is essentially zero. In fact, λ_c is a measurement of the optical band gap, since photons with a smaller wavelength than λ_c are absorbed by the sample exciting an electron from the valence band to the conduction band [24]. Moreover, the transmittance spectra of Fig. 5a–c exhibit a red shift of λ_c for samples with a low-temperature oxidation, while a blue shift is observed when the oxidation temperature is higher than 700 °C. In other words, there is a reduction followed by an enlargement of the optical band gap, when the thermal oxidation temperature grows. On the other hand, an oscillating behavior is found between 500 and 850 nm in Fig. 5a–e, which is a product of the multiple light reflection within the PSi film, and the oscillation amplitude is related to the refractive index of PSi film [25]. For example, this oscillation is negligible in Fig. 5f, since its refractive index is almost one. In fact, this free-standing sample was nearly transparent in the visible range.

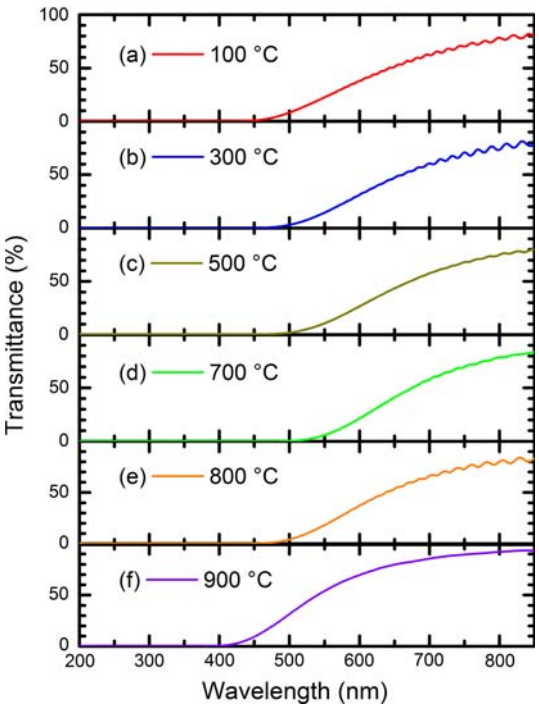

Fig. 5 **a–f** Optical transmittance spectra of free-standing PSi samples thermally oxidized at different temperatures indicated in the figures

Conclusions

We have presented a multi-approach study of the oxygen absorption in p^+-type free-standing PSi. By means of nitrogen adsorption, we were able to determine the average pore radius and surface area of the samples. These samples were also analyzed by the TGA technique, and both dynamic and isotherm analysis reveals the existence of an optimal oxygen-absorption temperature around 700 °C. Furthermore, the TGA analysis suggests a possible sintering process at 400 °C, which was elucidated by AFM structural observations. In fact, the red shift of optical transmittance spectra obtained from samples heated below 700 °C is in agreement with such sinterization, since growth of nanoclusters due to the sinterization leads to a diminish of the quantum confinement, in consequence a smaller optical band gap. It is important to emphasize that the temperatures found in this study could depend on the pore morphology and heating environment, for example, a sintering temperature of 1,000 °C is found in macroporous silicon [26] or 400 °C for mesopores as in this work.

Based on the XRD results, it could be assumed that O_2 absorption on PSi occurs throughout different mechanisms. While the PSi samples formed by interconnected *c*-Si nanostructures are heated, part of these convert into amorphous and polycrystalline Si, if temperature is about 500 °C. At higher temperatures, the diffusion of oxygen in PSi becomes important, and these three Si structures (crystalline, polycrystalline and amorphous) absorb it, producing SiO_2. The formation of crystalline SiO_2 proposed by XRD data is consistent with the blue shift of optical transmittance spectra at 800 and 900 °C, since the

optical band gap of crystalline SiO_2 is about 8.4 eV. Finally, the results suggest that O_2 absorption at low and high temperatures is respectively determined by sintering and diffusion processes.

Acknowledgments We gratefully acknowledge the technical assistance of Adriana Tejeda and Carlos Flores, as well as many stimulating discussions with Adriana Cázares. This work was partially supported by ICyT-DF-179/2009, CONACyT-58938 and PAPIIT-UNAM (IN114008 and IN100609).

References

1. L.T. Canham, Appl. Phys. Lett. **57**, 1046 (1990)
2. J. Liu, F. Liu, K. Gao, J. Wu, D. Xue, J. Mater. Chem. **19**, 6073 (2009)
3. J. Liu, H. Xia, D. Xue, L. Lu, J. Am. Chem. Soc. **131**, 12086 (2009)
4. C. Yan, D. Xue, Adv. Mater. **20**, 1055 (2008)
5. S. Chan, P.M. Fauchet. Appl. Phys. Lett. **75**, 274 (1999)
6. L.T. Canham, Adv. Mater. **7**, 1033 (1995)
7. L.M. Peter, D.J. Riley, R.I. Wielgosz, Appl. Phys. Lett. **66**, 2355 (1995)
8. J. Charrier, A. Alaiwan, P. Pirasteh, A. Najar, M. Gadonna, Appl. Surf. Sci. **253**, 8632 (2007)
9. H. Song, Z. Li, H. Chen, Z. Jiao, Z. Yu, Y. Jin, Z. Yang, M. Gong, X. Sun, Appl. Surf. Sci. **254**, 5655 (2008)
10. J. Liu, D. Xue, Adv. Mater. **20**, 2622 (2008)
11. A.E. Pap, K. Kordás, G. Tóth, J. Levoska, A. Uusimäki, J. Vähäkangas, S. Leppävuori, Appl. Phys. Lett. **86**, 041501 (2005)
12. B. Urbach, E. Axelrod, A. Sa'ar, Phys. Rev. B **75**, 205330 (2007)
13. V. Chamard, C. Pichat, G. Dolino, Eur. Phys. J. B **21**, 185 (2001)
14. E. Vázquez, J. Tagüeña-Martínez, L.E. Sansores, C. Wang, J. Appl. Phys. **91**, 3085 (2002)
15. R. Cisneros, C. Ramírez, C. Wang, J. Phys. Condens. Mat. **19**, 395010 (2007)
16. J.B. Condom, *Surface Area and Porosity Determinations by Physisorption* (Elsevier, Amsterdam, 2006), p. 6
17. F. Rouquerol, J. Rouquerol, K. Sing, *Adsorption by Powders and Porous Solids: Principles, Methodology and Applications* (Academic Press, London, 1999), p. 97
18. E.P. Barrett, L.G. Joyner, P.P. Halenda, J. Am. Chem. Soc. **73**, 373 (1951)
19. K.L. Jarvis, T.J. Barnes, A. Badalyan, P. Pendleton, C.A. Prestidge, J. Phys. Chem. C **112**, 9717 (2008)
20. B. Coasne, A. Grosman, C. Ortega, M. Simon, Phys. Rev. Lett. **88**, 256102 (2002)
21. I. Alcérreca-Corte, E. Fregoso-Israel, H. Pfeiffer, J. Phys. Chem. C **112**, 6520 (2008)
22. A.Wolf, R. Brendel, Thin Solid Films **513**, 385 (2006)
23. Y.H. Ogata, N. Yoshimi, R. Yasuda, T. Tsuboi, T. Sakka, A. Otsuki, J. Appl. Phys. **90**, 6487 (2001)
24. J. Singh, K. Shimakawa, *Advances in Amorphous Semiconductors* (Taylor & Francis, London, 2003), p. 61
25. P. Yeh, *Optical Waves in Layered Media* (John Wiley, New York, 2005), p. 90
26. H. Seel, R. Brendel, Thin Solid Films **451**, 608 (2004)